J Oceanogr (2011) 67:601–611
DOI 10.1007/s10872-011-0060-1

ORIGINAL ARTICLE

Seasonal variation of eddy shedding from the Kuroshio intrusion in the Luzon Strait

Yinglai Jia · Eric P. Chassignet

Received: 1 November 2010 / Revised: 21 June 2011 / Accepted: 5 July 2011 / Published online: 10 August 2011

Abstract Altimeter data and output from the HYbrid Coordinate Ocean Model global assimilation run are used to study the seasonal variation of eddy shedding from the Kuroshio intrusion in the Luzon Strait. The results suggest that most eddy shedding events occur from December through March, and no eddy shedding event occurs in June, September, or October. About a month before eddy shedding, the Kuroshio intrusion extends into the South China Sea and a closed anticyclonic eddy appears inside the Kuroshio loop which then detaches from the Kuroshio intrusion. Anticyclonic eddies detached from December through February move westward at a speed of about 0.1 m s^{-1} after shedding, whereas eddies detached in other months either stay at the place of origin or move westward at a very slow speed (less than 0.06 m s^{-1}). The HYCOM outputs and QuikSCAT wind data clearly show that the seasonal variation of eddy shedding is influenced by the monsoon winds. A comparison between eddy volume and integrated Ekman transport indicates that, once the integrated Ekman transport exceeds 2×10^{12} m^3 (which roughly corresponds to the volume of an eddy), the Kuroshio intrusion expands and an eddy shedding event occurs within 1 month. We infer that the Ekman drift of the northeasterly monsoon pushes the Kuroshio intrusion into the SCS, creates a net westward transport into the Strait, and leads to an eddy detachment from the Kuroshio.

Keywords Eddy shedding · Kuroshio intrusion · Luzon Strait · Seasonal variation

Y. Jia (✉)
Physical Oceanography Laboratory, Ocean University of China, Qingdao, China
e-mail: jiayingl@ouc.edu.cn

Y. Jia · E. P. Chassignet
Center for Ocean-Atmospheric Prediction Studies, Florida State University, Tallahassee, USA

1 Introduction

The Luzon Strait, with an average width of around 400 km and an average depth of over 2,000 m, is the main gap in the western boundary of the North Pacific. The Kuroshio, the western boundary current of the North Pacific, deforms while crossing the Luzon Strait. The deformation of the Kuroshio, with temporal and spatial variation, results in anticyclonic eddy shedding. Gaining some insight into the variability of eddy shedding phenomena will lead to a better understanding of the temporal variation in water exchange between the South China Sea (SCS) and the Pacific Ocean. The transport of warm and salty water into the SCS is vital to the ecosystem and to the fisheries, so it is important to understand the characteristics and variability of the eddy shedding phenomena.

Several studies have examined the eddy shedding and the Kuroshio intrusion in the Luzon Strait (Yuan et al. 2006; Metzger and Hurlburt 2001; Liang et al. 2008). There appears to be consensus that the Kuroshio intrusion does not exhibit a clear seasonal cycle. They also point out that, while there is a clear relationship between a Kuroshio extension and an eddy shedding event, it is a necessary condition, but not sufficient. Jia and Liu (2004) used AVISO altimetry data combined with a modeled mean of sea surface height (SSH) and found that anticyclonic eddies periodically separate from the Kuroshio intrusion with an average shedding time of 70–90 days, with no significant

seasonal variation. However, the mean SSH they used featured a permanent Kuroshio loop that may have contaminated their conclusions. Observations show that the Luzon Strait Transport (LST) is stronger in winter than in summer (Shaw 1991; Qu et al. 2000; Liang et al. 2008) and may induce a seasonal variation in eddy shedding. So far, the presence of a seasonal signal in eddy shedding in the Luzon Strait remains unclear.

Very few studies have addressed the mechanism of eddy shedding in the Luzon Straits. Jia et al. (2005) examined instabilities in the Kuroshio front in model results and found that frontal instability in the Kuroshio intrusion causes the separation of anticyclonic eddies from the Kuroshio. Sheremet (2001) examined the hysteresis phenomena in inertial flow and suggested eddy shedding is a transition phenomenon that happens when the Kuroshio changes from the leaping mode to the penetrating mode. However, none of these works included any wind effect on Kuroshio intrusion and eddy shedding. Using observational data, Farris and Wimbush (1996) surmised that the expanding of the Kuroshio loop is controlled by the time-integrated wind stress.

In this paper, we further examine the seasonal variation of eddy shedding from the Kuroshio intrusion in the Luzon Strait using altimetry observation and outputs of the HYbrid Coordinate Ocean Model (HYCOM) global assimilation run (Chassignet et al. 2009), and investigate the relationship between eddy shedding and wind-induced Ekman transport. We show that there is seasonality in the eddy shedding and that it is consistent with a stronger LST (Liang et al. 2008) and with the integrated monsoon-induced Ekman transport. The latter is supported by the numerical experiments of Metzger and Hurlburt (1996) and Zhao et al. (2009) who showed that the variation of LST is very weak without a local seasonal variation in the wind. This suggests that, although the Ekman induced transport by the wind is much smaller than the LST, the winter monsoon wind is able to push the Kuroshio intrusion into the SCS to form stronger LST in winter as suggested by Farris and Wimbush (1996). We find that, when the integrated Ekman transport exceeds 2×10^{12} m^3 (which roughly corresponds to the volume of an eddy), the Kuroshio loop expands and an eddy shedding event occurs within 1 month.

The layout of the paper is as follows. In Sect. 2, we briefly introduce the observations and the model outputs. Section 3 first investigates the impact of the choice of the mean SSH and then documents the seasonal variation and characteristics of eddy shedding in the Luzon Strait. The relationship between eddy shedding and Kuroshio transport as well as Ekman transport by local wind is explored in Sect. 4. The final section presents the conclusions of the study.

2 Data and model outputs

2.1 SSH anomaly

The primary observations used to investigate the seasonal variation of the eddy shedding from the Kuroshio in the Luzon Strait are SSH anomalies from altimetry observations. The SSH anomaly datasets were obtained from AVISO at 7-day intervals, with a 1/3° × 1/3° resolution gridded to a Mercator projection for the period 1993–2009. This dataset combines sea surface altimetry from Topex/Poseidon, ERS-1, ERS-2, Jason-1, and ENVISAT (depending on availability), into a product of merged sea level anomaly (AVISO 2006).

2.2 Mean dynamic topography

In order to get the total SSH, the above anomalies need to be combined with a mean. The mean dynamic topographies (MDTs) used in this paper are derived from the following four data sources: (1) the mean dynamic topography for the period 1992–2002 with 0.5° resolution calculated using the large-scale mean sea level from the GRACE satellite and mesoscale sea level tilt derived from drifter, satellite altimeter, and wind data (Maximenko and Niiler 2005); (2) the mean dynamic topography for the period 1993–1999 with 0.25° resolution of CNES-CLS09 calculated from altimetry and a geoid model (Rio et al. 2009); (3) the mean dynamic topography for the period from November 2003 to September 2009 from the HYCOM model with 1/12° resolution (Chassignet et al. 2009); and (4) the mean dynamic topography for the period 1992–1996 from the Parallel Ocean Climate Model (POCM) output (Semtner and Chervin 1992) with 0.25° resolution. Of these four data sources, only the fourth was used by Jia and Liu in their 2004 study.

2.3 HYCOM SSH and velocity

The SSH and velocity data are from the HYCOM global assimilation run (Chassignet et al. 2009). These data are on a 1/12° global grid (mid-latitude resolution of ~7 km) with 32 hybrid vertical coordinate surfaces. The global assimilation output is based on a fully 3-D multivariate optimum interpolation scheme in the HYCOM model to assimilate observational data, including altimeter SSH anomalies and other observations. The time span of the data is from November 2003 to September 2009 with 1-day intervals.

2.4 Surface wind

The surface wind data used in this study are from QuikSCAT with 0.25° × 0.25° resolution at 1-day intervals for the period from July 1999 to September 2009. Wind stress

is calculated from QuikSCAT wind speed and direction data (Perry 2001).

3 Seasonal variation and characteristics of eddy shedding in the Luzon Strait

As a first step in investigating the question as to whether there is indeed seasonal variation in the eddy shedding phenomena, the four MDTs described in Sect. 2.1 are compared and their use in combination with AVISO SSH anomalies is discussed (Sect. 3.1). A specific example of a winter eddy shedding is then described in Sect. 3.2 in order to provide some insights into the separation process. Finally, the seasonal variation of eddy shedding is discussed using both the altimetry observations and HYCOM outputs (Sect. 3.3).

3.1 The impact of choice of the mean SSH

Three of the MDTs agree with each other, the two derived from observations, Max05 (Maximenko and Niiler 2005) (Fig. 1a) and CNES-CLS09 (Rio et al. 2009) (Fig. 1b), and the HYCOM mean (Fig. 1c). In these MDTs, the Kuroshio intrusion is located east of 119°E in good agreement with a 15-year mean derived from shipboard ADCP observations (Liang et al. 2008). In the HYCOM mean, the SSH gradient across the Luzon Strait is a somewhat greater than that in the observational means.

In the POCM mean (Fig. 1d), however, the Kuroshio intrusion extends almost all the way to 118°E, which is about 1° west of the intrusion as measured from observations. We therefore hypothesize that the deep intrusion of the Kuroshio in the POCM mean can merge with local anticyclonic eddies in the SCS, a process that can lead to an inaccurate number of eddy shedding events in summer. This is illustrated in Fig. 2 which displays the same series of events in June 1996 using AVISO anomalies with the POCM and HYCOM MDTs, respectively. In the POCM SSH fields (Fig. 2a, c, e, g), one can see a local eddy merge with the Kuroshio extension while the same eddy in the HYCOM fields remains unattached. On June 5, 1996, an anticyclonic eddy is located in both the POCM and

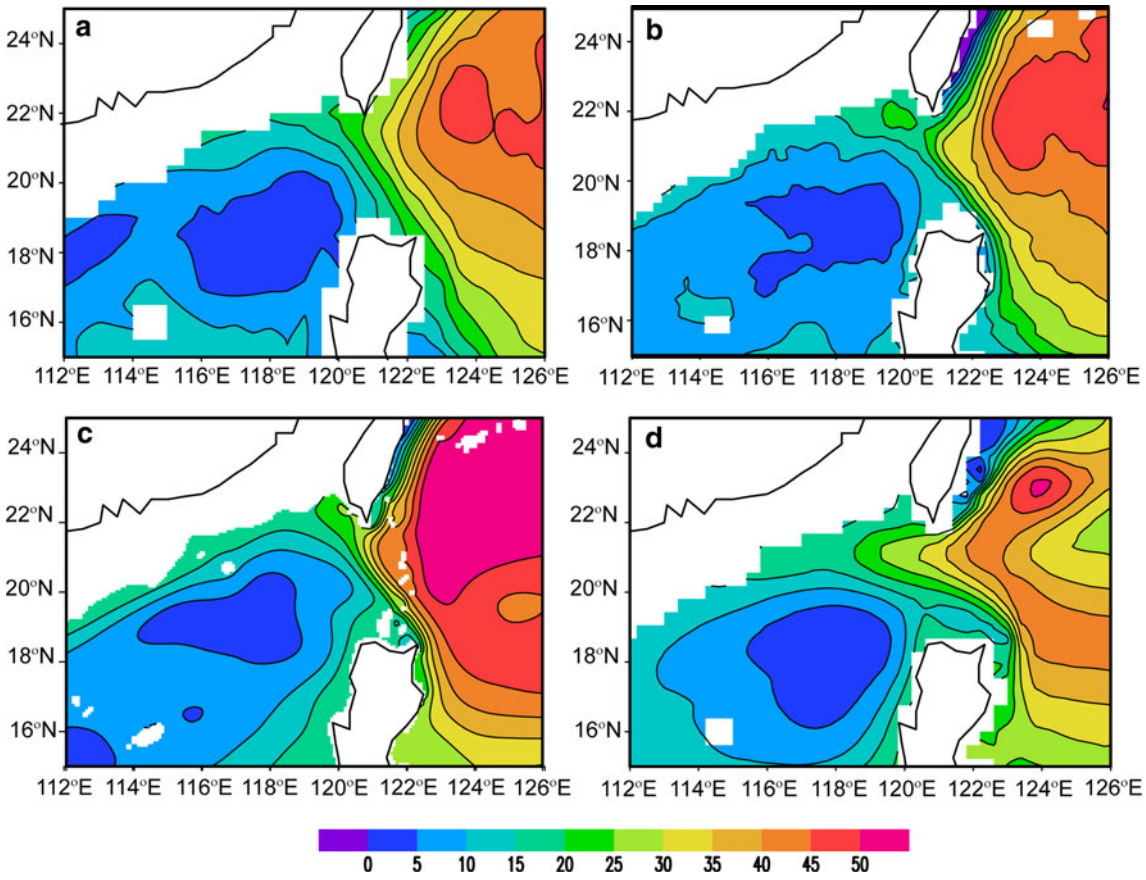

Fig. 1 Mean SSH from **a** mean ocean dynamic topography of Max05 (mean of 1992–2002) (Maximenko and Niiler 2005), **b** MODT of CNES-CLS09 (mean of 1993–1999) (Rio et al. 2009), **c** HYCOM result (mean of 2003–2009), **d** POCM model result (mean of 1992–1996). Area shallower than 150 m is blocked. For easy comparison of the gradient between these data, the averaged SSH in the domain was subtracted from the mean SSH and a constant was added to move the minimum SSH value to zero. Unit: cm

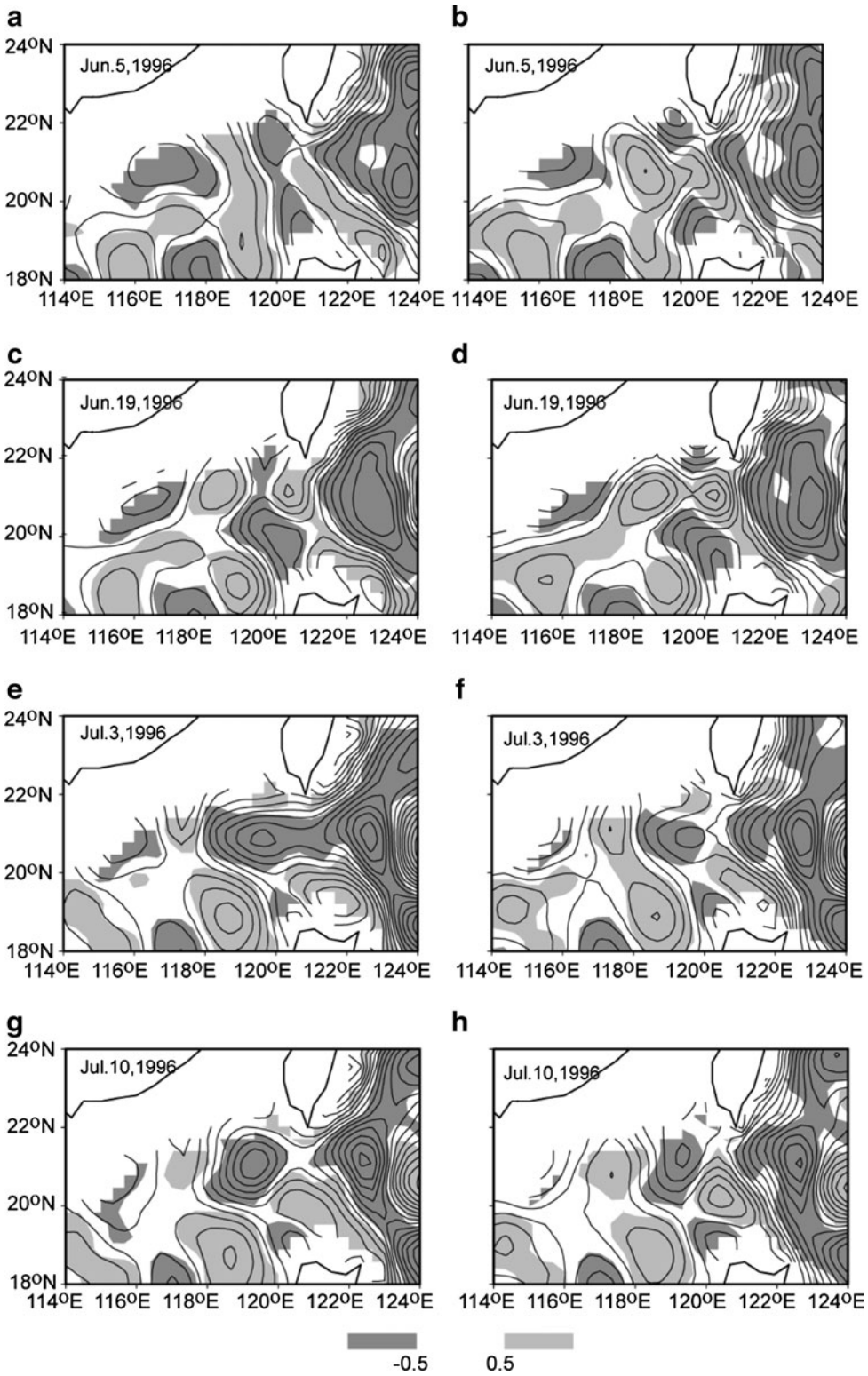

Fig. 2 SSH contours from altimetry data with POCM mean (*left panel*) and with HYCOM mean (*right panel*). Contour interval for SSH is 5 cm. *Shading* is geostrophic vorticity calculated from the SSH. Unit of geostrophic vorticity is 1×10^{-6} s^{-1}. Areas shallower than 150 m are blocked

HYCOM SSH fields (Fig. 2a, b). According to Yuan et al. (2007), this is a SCS local eddy, called a Luzon warm eddy, which normally forms northwest of Luzon Island in the summer and then moves northwestward. Between June 19 and July 3, 1996, the Kuroshio intrusion expands westward to 118°E (Fig. 2c) and then develops into a full Kuroshio loop as the result of the merging of the warm eddy with mean SSH (Fig. 2e). In the HYCOM SSH fields, although the Kuroshio intrusion did expand westward, it remains confined east of 120°E (Fig. 2d, f). After 2 weeks,

on 10 July 1996, an eddy shedding event appears to have occurred in the POCM SSH field (Fig. 2g). By comparison, the local warm Luzon eddy in the HYCOM SSH fields remains separated (Fig. 2h). This example shows how the large Kuroshio loop in the mean SSH from the POCM model can merge with local summer Luzon eddies and cause misidentification of eddy shedding events during summer (Jia and Liu 2004). In winter, local eddies around the Kuroshio intrusion are mostly cyclonic and therefore do not have much influence on the number of eddy shedding events identified for the winter.

This comparison shows that the extent and location of the Kuroshio intrusion in the mean SSH is important for the identification of eddy shedding. Since the pattern of Kuroshio intrusion in the HYCOM output displays most of the features of the Kuroshio intrusion in the observations (Liang et al. 2008), the AVISO altimetry observation with the HYCOM mean will be used to study eddy shedding phenomena discussed in later sections of this study. Furthermore, since the AVISO data can only provide information about the ocean surface, the HYCOM model output (including velocity and SSH), with its higher spatial and temporal resolution, will also be used in studying the eddy shedding process.

3.2 Separation process of an anticyclonic eddy in winter

In this section, an example of eddy shedding in winter is discussed using both altimetry data with the HYCOM MDT and HYCOM outputs (SSH and total velocity) in order to investigate the eddy shedding process from the Kuroshio in the Luzon Strait.

The HYCOM outputs used here are from the global run with data assimilation (Chassignet et al. 2009). Altimetry is assimilated along tracks and the correlation coefficient between the SSH anomaly from AVISO and the HYCOM global run from 2003 to 2009 is higher than 0.6 in most of the SCS and in the Pacific (Fig. 3). The correlation coefficient is, however, quite low in the northern Luzon Strait where the Kuroshio curves toward the SCS and where Kuroshio intrusion and eddy shedding occur. This is not surprising given the inaccuracy of altimetry near the shore and the objective mapping used by AVISO. The difference may be due to more eddies, and more variation in those eddies, being visible because of the higher resolution in the HYCOM model (see interpretations in Sect. 3.3).

Figure 4 shows an example of eddy shedding in the Luzon Strait in winter. Following the method outlined in Jia and Liu (2004), geostrophic vorticity is calculated from the HYCOM AVISO SSH in order to facilitate the detection of anticyclonic eddies. For this specific example, the Kuroshio intrusion began developing on January 14, 2004,

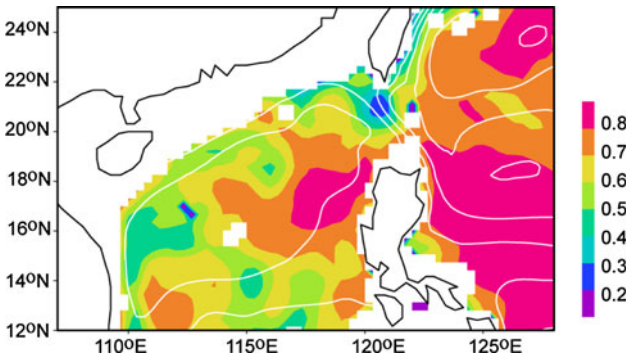

Fig. 3 Correlation coefficient between AVISO-HYCOM SSH and HYCOM SSH. *White contour* is the mean SSH of HYCOM output

and took about 20 days to extend to 118.5°E; a loop then appeared on February 4, 2004. An anticyclonic eddy formed in the loop and separated from it on 11 February 2004. Located at 21°N, 118.5°E, with a dimension of 200 km in longitude and 150 km in latitude, this anticyclonic eddy had a meridional speed of about 0.3 m s^{-1} along 21.5°N, and a maximum surface geostrophic vorticity of 8×10^{-6} s^{-1} (the surface geostrophic vorticity is calculated from the SSH, the corresponding vorticity at 100 m is much higher values on the order of 3×10^{-5} s^{-1}). After the eddy shedding event on 11 February 2004, the detached anticyclonic eddy moved westward at a speed of about 0.1 m s^{-1} while the Kuroshio was mainly confined east of 120°E. The lifetime of this eddy was about 30 days before it moved past Dongsha Island (about 21°N, 117°E) and dissipated. The depictions of the Kuroshio intrusion in the HYCOM model outputs and in the HYCOM AVISO altimetry were in phase and the location and movement of the detached eddy were also in agreement. These results agree with those of Wang et al. (2008), who captured the same anticyclonic eddy by in situ observation. Their analysis of the temperature-salinity scatter diagrams proved that this anticyclonic eddy separated from the Kuroshio (see their Figs. 2 and 9).

3.3 Seasonal characteristics of eddy shedding

We now explore the seasonal variation of eddy shedding in the Luzon Strait. The occurrence of eddy shedding in different months will be examined, and the diameter, maximum velocity, and migration speed of the eddies will be discussed. Both the HYCOM AVISO altimetry observations and HYCOM outputs will be used to study the characteristics of eddy shedding.

The eddy shedding events that occurred during the period 1993–2009 are documented in Table 1 together with their characteristic features. The eddy shedding time is defined as the date a closed anticyclonic vorticity and SSH

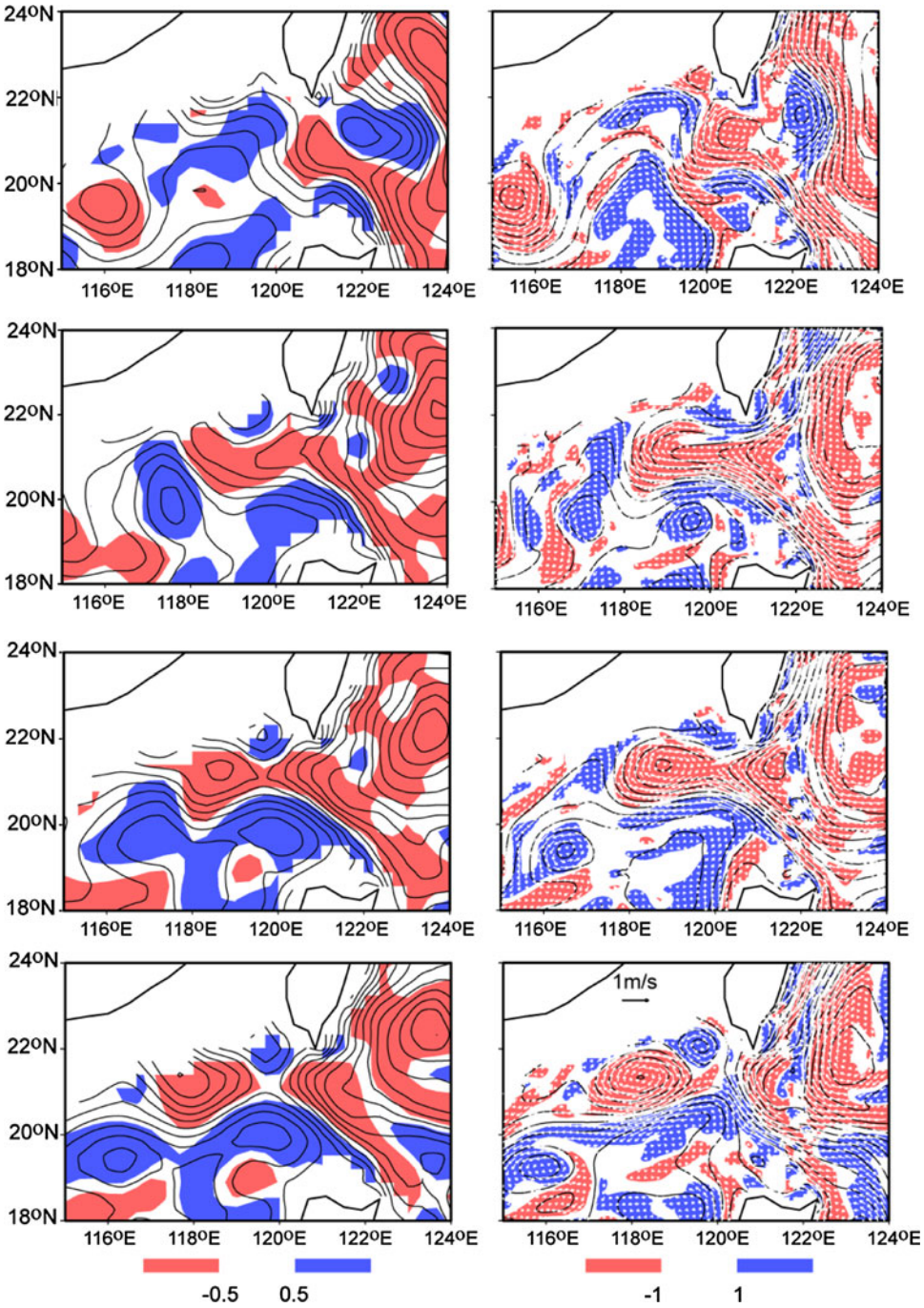

Fig. 4 SSH and geostrophic vorticity through January to March 2004 from AVISO-HYCOM data (*left panel*) and from HYCOM output (*right panel*). *Contours* are SSH and *shading* is geostrophic vorticity. The *vectors in the right panel* represent the velocity at 100 m depth from HYCOM output. Contours in areas shallower than 150 m are not plotted. The contour interval for the SSH is 5 cm. *Red (blue) shaded areas* are for geostrophic vorticity greater (*lower*) than $+(-)0.5 \times 10^{-6}$ s^{-1} (*left panel*) or $+(-)1 \times 10^{-6}$ s^{-1} (*right panel*)

contour appeared inside the Kuroshio loop. The diameter is the zonal extent the eddy occupied in the SSH field. The maximum velocity is based on the geostrophic velocity calculated from the SSH. The migration speed is calculated from the zonal distance (the distance moved before disappearance) divided by the time it took to travel the distance.

The HYCOM AVISO altimetry shows that, during the period 1993–2009, 15 eddy shedding events occurred in winter monsoon period (from November to the following April) and 3 occurred in summer monsoon period (from May to October). According to the results from the altimetry observation, eddy shedding is roughly an annual event. The exception is in 2000, when four eddy shedding events occurred. In 1995, 2003, 2006, and 2008–2009, no eddy shedding event is found using the HYCOM AVISO altimetry observation. These differences suggest that strong inter-annual variation exists in the eddy shedding phenomena. During the period of November 2003–November 2009, the data assimilative HYCOM outputs show that

Table 1 Features of eddy shedding in the Luzon Strait (AVISO observation and HYCOM result) (May to October is defined as summer and other months as winter)

Date (winter or summer)	Location AVISO	Diameter/velocity/ migration speed			Location HYCOM	Diameter/velocity/ migration speed		
Dec 30, 1992 (W)	21.0°N, 119.5°E	150	0.3	0.09				
Mar 24, 1993 (W)	20°N, 119°E	100	0.1	0				
Dec 07, 1994 (W)	21.5°N, 119.5°E	150	0.3	0				
Mar 13, 1996 (W)	21.5°N, 119.5°E	200	0.35	0				
Dec 04, 1996 (W)	21°N, 119.5°E	200	0.4	0.05				
Dec 31, 1997 (W)	21.5°N, 118.5°E	200	0.35	0.16				
Jul 08, 1998 (S)	21.5°N, 118.5°E	100	0.1	0.04				
Apr 28, 1999 (W)	21.5°N, 119.5°E	150	0.2	0				
Feb 09, 2000 (W)	21.5°N, 119°E	200	0.3	0.15				
May 17, 2000 (S)	22°N, 119°E	150	0.15	0.05				
Jul 19, 2000 (S)	22°N, 119°E	200	0.35	0				
Dec 27, 2000 (W)	21.5°N, 118.5°E	150	0.2	0				
Nov 28, 2001 (W)	22°N, 119.5°E	100	0.1	0				
Feb 11, 2004 (W)	21°N, 118°E	200	0.25	0.09	21.5°N, 118.5°E	200	0.4	0.11
Apr 05, 2004 (W)					21.5°N, 119.5°E	200	0.4	0
Aug 02, 2004 (S)					21°N, 120.5°E	100	0.4	0.06
Dec 08, 2004 (W)	21.5°N, 119.5°E	200	0.3	0.1				
Dec 16, 2004 (W)					21.5°N, 119°E	200	0.45	0.1
Mar 02, 2005 (W)	21.5°N, 119°E	100	0.25	0	21.5°N, 120°E	200	0.3	0
Mar 05, 2006 (W)					22°N, 120°E	100	0.2	0
Jan 10, 2007 (W)	21.5°N, 119.5°E	200	0.3	0.1	21°N, 120°E	150	0.3	0.11
Dec 26, 2007 (W)	21°N, 119°E	100	0.2	0.06	22°N, 119°E	100	0.5	0.11
May 08, 2009 (S)					22°N, 119.5°E	150	0.35	0.05
	15 in winter, 3 in summer				7 in winter, 2 in summer			

The unit of diameter is km, velocity is m s^{-1}, and migration speed is m s^{-1}

seven eddy shedding events occurred in winter monsoon period and two occurred in summer monsoon period. More eddy shedding events are detected in the HYCOM outputs than in the HYCOM AVISO altimetry during the period November 2003–November 2009 (Table 1), possibly because of the finer spatial and temporal resolution in the data assimilative model. The more frequent eddy shedding phenomena in the Luzon Strait in the HYCOM outputs indicate there are more eddy activities in the Luzon Strait in SSH fields from HYCOM data than from altimetry observation. This would explain the drop in the correlation coefficient (Fig. 3) between the SSH from altimetry and the SSH from HYCOM data in the Luzon Strait.

The occurrence of eddy shedding by month is summarized in Fig. 5. Eddy shedding is most prevalent in December, followed by March. No eddies were shed in June, September, or October. This result shows that eddy shedding tends to occur when the northeast monsoon wind prevails and when Kuroshio intrusion is stronger into the SCS.

The diameters and the maximum velocities of anticyclonic eddies in summer and winter are summarized in Fig. 6. The most frequently occurring diameter of anticyclonic eddies is 200 km, and eddies with this characteristic appear mostly in winter. In the altimetry observation, the maximum velocity of over half of the anticyclonic eddies exceeds 0.3 m s^{-1}, and eddies with this characteristic occur mostly in winter. In the HYCOM outputs, the maximum velocity can exceed 0.5 m s^{-1} in winter, possibly indicating stronger eddies if one considers that ageostrophic flows are weak. Both the HYCOM AVISO altimetry and HYCOM outputs indicate eddies are larger and stronger in winter than in summer. This may be related to the stronger LST in winter (Liang et al. 2008).

As shown in Table 1, from both data sources, most of the eddies separated in the period from December through February move westward at a speed of about 0.1 m s^{-1} after detaching, which is much higher than the first baroclinic Rossby wave speed in the northern SCS (0.05 m s^{-1}; Cai et al. 2008). The migration speed of these eddies agrees with the findings by Wang et al. (2008). Eddies that separated in March–April will stay at the place of origin until they dissipate. March–April is spring in the SCS, and the

northeasterly monsoon is weaker than it is in winter. Eddies separating in summer may stay at the place of origin or move westward at a very slow speed (0.05–0.06 m s^{-1}).

In summary, winter is the most favorable season for eddy shedding from the Kuroshio in the Luzon Strait. The anticyclonic eddies detached in winter are stronger than those detached in summer. Eddies detached from December through February move westward at a speed of about 0.1 m s^{-1} after shedding, whereas eddies detached in other months either stay at the place of origin or move westward at a very slow speed (less than 0.06 m s^{-1}). The high migration speed of detached eddies was explained as being wind-induced by Nof et al. (2011) using analytical theory and numerical models. The latter also suggests that the mechanism of eddy shedding may be related to the seasonally varying monsoon wind. Earlier studies (Jia et al. 2005; Sheremet 2001) have suggested that the Kuroshio transport may also have a close relationship with eddy shedding. For a better understanding of the mechanism of eddy shedding, the relationship of eddy shedding to the Kuroshio transport and the monsoon wind will be examined in the following section.

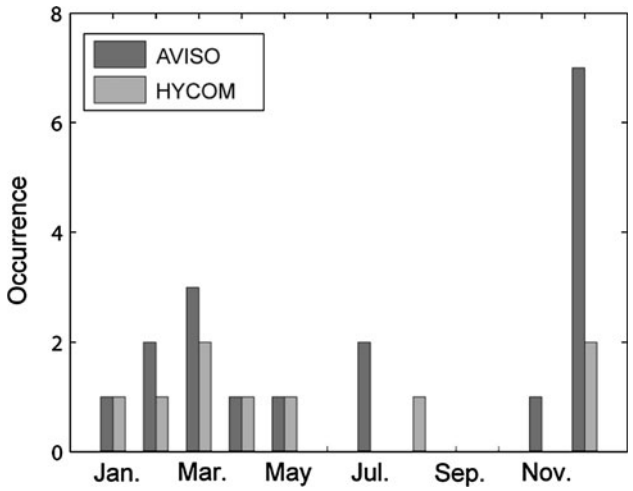

Fig. 5 The occurrence of anticyclonic eddy shedding in different months. *Dark gray bar* is the occurrence in AVISO observation. *Light gray bar* is the occurrence in HYCOM output

4 Relationship with Kuroshio transport and Ekman effect of local wind

The relationship between eddy shedding and Kuroshio transport is further investigated using the HYCOM outputs and QuikSCAT wind data. The Kuroshio transport is calculated from meridional velocity in the upper 400 m across 18.5°N between 122 and 124°E (Fig. 7). Intra-seasonal—rather than seasonal—variations are found to be the most significant signal in agreement with previous studies. Eddy shedding events can, however, be found to occur more frequently when the Kuroshio transport variability is high (see, for example, the February 2004–March 2005 period). One does not expect a simple relationship between the Kuroshio transport and eddy shedding because of the hysteresis present in the dynamics of Kuroshio (Sheremet 2001).

It has been suggested by Farris and Wimbush (1996) that local winds have a direct effect on Kuroshio intrusion and that the expansion of the Kuroshio loop is largely determined by the time integrated wind stress in the Luzon Strait. The latter is supported by the numerical experiments of Metzger and Hurlburt (1996) and Zhao et al. (2009) which show that the variations in the LST are very weak without local seasonal variation in the wind. In order to quantify the effect of local winds, the Ekman transport flowing into the Luzon Strait is calculated along 121.75°E using the QuikSCAT wind data. Figure 8a shows that from November 2003 to September 2009, the eddy shedding in the HYCOM simulation occur mostly in winter when there is a stronger Ekman-induced transport flow into the Strait. This suggests that the eddy shedding is facilitated by the presence of northeasterly winds and that although the Ekman induced transport by the wind is much smaller than the LST, the winter monsoon wind is able to push the

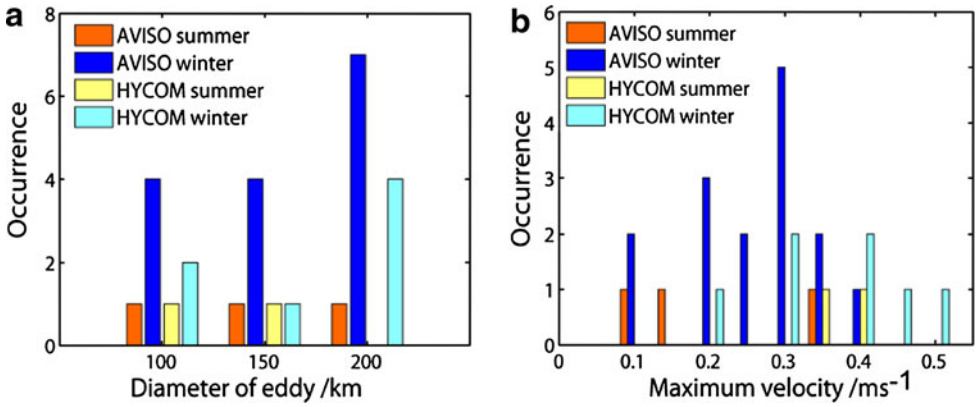

Fig. 6 **a** The occurrence of diameter of anticyclonic eddy. **b** The occurrence of maximum velocity in the anticyclonic eddy. *Blue* and *orange bars* are the occurrence in winter and summer from AVISO observation, respectively. *Light blue* and *yellow bars* are the occurrence in winter and summer from HYCOM output, respectively

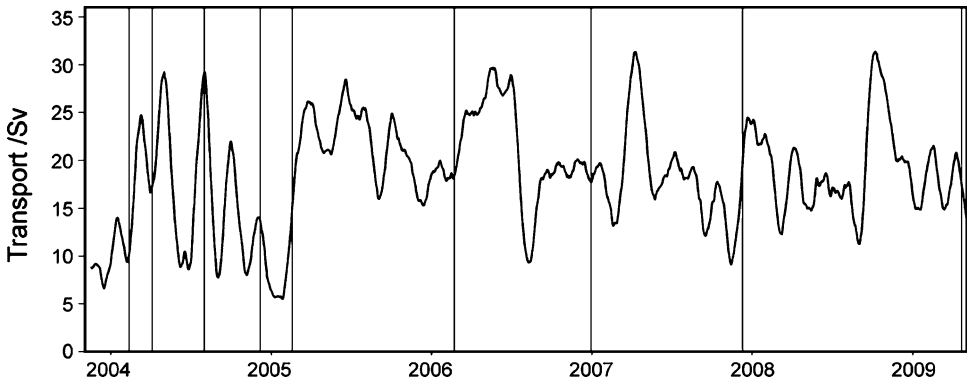

Fig. 7 Kuroshio transport during 2003–2009 in the upper 400 m across 18.5°N from HYCOM output. *Positive values* represent northward transport. A 30-day running mean was applied. Unit: Sv. *Straight lines* mark the HYCOM eddy shedding times according to Table 1. *Time-axis tick marks* indicate the beginnings of the designated years

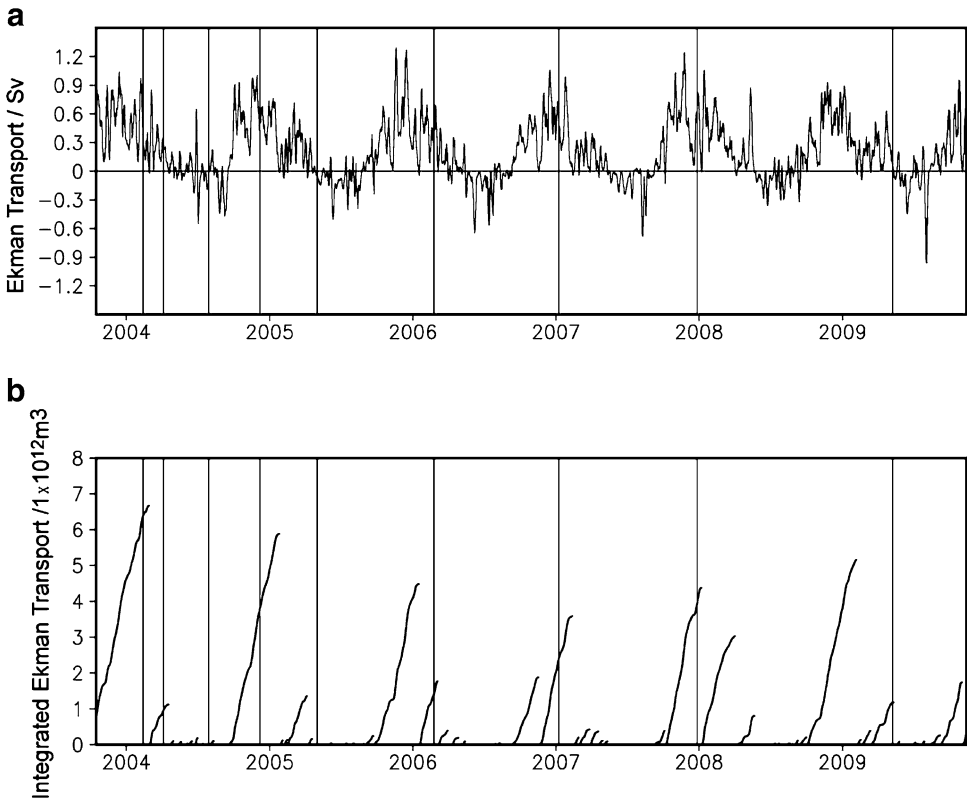

Fig. 8 **a** Zonal Ekman transport across 121°E from 19°N to 22°N during 2003–2009 in the Luzon Strait from QuikSCAT wind data. A 5-day running mean was applied. *Positive values* represent westward transport. Unit: Sv. *The horizontal straight line* is the zero line. **b** Time integrated Ekman transport. Unit: 1×10^{12} m^3. The time-integrated Ekman transport is calculated from the positive zonal Ekman transport (i.e., into the Luzon Strait) from January 2003 to September 2009. When the Ekman transport changes from positive to negative, the integrated Ekman transport is reset to zero. As the time axis starts from November 2003, the integrated Ekman transport is non-zero at the start of the axis. The *vertical straight lines* in (**a**) and (**b**) mark the HYCOM eddy shedding time according to Table 1. *Time-axis tick marks* indicate the beginnings of the designated years

Kuroshio intrusion into the SCS to strengthen the LST as suggested by Farris and Wimbush (1996). We find that when the integrated Ekman transport exceeds 2×10^{12} m^3 (Fig. 8b), the Kuroshio loop expands and eddy shedding event occurs within 1 month. 2×10^{12} m^3 roughly corresponds to the volume of an eddy of radius $R = 100$ km and relative vorticity $\zeta = 3 \times 10^{-5}$ s^{-1} using Nof's (2005) formula $\left(V = \frac{\zeta}{f}\left(2 - \frac{\zeta}{f}\right)\pi f^2 R^4 / 16g'\right)$. From November 2003 to April 2004, the integrated Ekman transport is 7×10^{12} m^3, which is the highest during the period 2003–2009 and corresponds to the detachment of three eddies that occurred sequentially in 2004. From October 2006 to July 2008, the integrated Ekman transport is relatively low (about 3–4 $\times 10^{12}$ m^3) and leads to only one eddy shedding each year. The only exception to the rule suggested above is from October 2008 to April 2009: during that time, the integrated Ekman transport is about 5×10^{12} m^3, but no eddy detached. From the SSH pattern in that winter (figure not shown), there was a strong cyclonic eddy west of Luzon Strait, which hindered the intrusion of the Kuroshio. Although we only have 9 cases of eddy shedding events during 2003–2009, 8 out of 9 cases indicate a close relationship between eddy shedding frequency and integrated Ekman transport into the Luzon Strait. These findings indicate that the seasonal variation of eddy shedding is influenced by the local monsoon wind and that the Ekman transport by the wind provides a necessary

source of transport into the Luzon Strait for eddies to detach from the Kuroshio.

5 Conclusions

Seasonal variation of eddy shedding from Kuroshio intrusion in the Luzon Strait is studied using AVISO SSH anomaly combined with HYCOM mean, and SSH and velocity from HYCOM global assimilation output. The correlation between SSH from HYCOM output and SSH from altimetry observation is higher than 0.6 in most of the regions around the Luzon Strait, which makes us confident in studying eddy shedding in the Luzon Strait using HYCOM output. From both data sources, eddy shedding events from the Kuroshio intrusion are visually determined from the SSH and geostrophic vorticity patterns. About a month after a Kuroshio intrusion extends into the SCS and forms a loop, a closed SSH contour appears inside the Kuroshio loop. An anticyclonic eddy then detaches from the Kuroshio intrusion. Most eddy shedding events occur from December through March, and no eddy shedding event occurs in June, September, or October. The anticyclonic eddies detached in winter tend to be larger and stronger than those detached in summer. Anticyclonic eddies detached from December through February move westward at a speed of about 0.1 m s^{-1} after shedding, whereas eddies detached in other months either stay at the place of origin or move westward at a slow speed (less than 0.06 m s^{-1}).

In winter, the SCS is controlled by the northeast monsoon wind. The Ekman effect of monsoon wind pushes the Kuroshio intrusion into the SCS, provides a net transport into the Strait, and contributes to the detachment of an eddy from the Kuroshio. Using HYCOM output and QuikSCAT wind data, a close relationship between eddy shedding frequency and integrated Ekman transport into the Luzon Strait is found. It indicates that after the integrated Ekman transport exceeding 2×10^{12} m^3, which is roughly the volume of an eddy, the Kuroshio loop extends and an eddy shedding event occurs within 1 month. These results are based on data analysis and statistical work. Numerical experiments are needed to provide further proof and to understand the mechanism of the wind effect on eddy shedding from the Kuroshio in the Luzon Strait.

Using a numerical model, Sheu et al. (2010) work suggest that eddies from the Pacific are likely to propagate through the Luzon Strait when the Kuroshio intrusion is strong in winter. It is worthwhile to investigate further whether these eddies from the Pacific influence eddy shedding.

Acknowledgments The authors thank the two anonymous reviewers for valuable comments and detailed suggestions to improve the manuscript. We thank Kathy Fearon for help with the English writing. The altimeter data are obtained from the Aviso Web site at http://www.aviso.oceanobs.com/en/data/index.html. Y. Jia is supported by Chinese National Key Basic Research Program (2007CB411803) and National Natural Science Foundation of China (40706005). E.P. Chassignet acknowledges the support of NSF grant OCE-0752225.

References

AVISO (2006) SSALTO/DUACS user handbook: (M)SLA and (M)ADT near-real time and delayed time products. Archiving, Validation and Interpretation of Satellite Oceanographic Data (AVISO), Ramonville St-Agne, France

Cai S, Long X, Wu R, Wang S (2008) Geographical and monthly variability of the first baroclinic Rossby radius of deformation in the South China Sea. J Mar Sys 74:711–720. doi:10.1016/j.jmarsys.2007.12.008

Chassignet EP, Hurlburt HE, Metzger EJ, Smedstad OM, Cummings J, Halliwell GR, Bleck R, Baraille R, Wallcraft AJ, Lozano C, Tolman HL, Srinivasan A, Hankin S, Cornillon P, Weisberg R, Barth A, He R, Werner F, Wilkin J (2009) U.S. GODAE: Global Ocean Prediction with the HYbrid Coordinate Ocean Model (HYCOM). Oceanography 22:64–75

Farris A, Wimbush M (1996) Wind-induced Kuroshio intrusion into the South China Sea. J Oceanogr 52:771–784

Jia Y, Liu Q (2004) Eddy shedding from the Kuroshio bend at Luzon Strait. J Oceanogr 60:1063–1069

Jia Y, Liu Q, Liu W (2005) Primary study of the mechanism of eddy shedding from the Kuroshio bend in Luzon Strait. J Oceanogr 61:1017–1027

Liang W, Yang Y, Tang T, Chuang W (2008) Kuroshio in the Luzon Strait. J Geophys Res 113:C08048. doi:10.1029/2007JC004609

Maximenko NA, PP Niiler (2005) Hybrid decade-mean global sea level with mesoscale resolution. In: N. Saxena (ed) Recent advances in marine science and technology. PACON International, Honolulu, pp 55–59

Metzger EJ, Hurlburt HE (1996) Coupled dynamics of the South China Sea, the Sulu Sea and the Pacific Ocean. J Geophys Res 101:12331–12352

Metzger EJ, Hurlburt HE (2001) The nondeternimistic nature of Kuroshio penetration and eddy shedding in the South China Sea. J Phys Oceanogr 31:1712–1732

Nof D (2005) The momentum imbalance paradox revisited. J Phys Oceanogr 35:1928–1939

Nof D, Jia Y, Chassignet E, Bozec A (2011) Fast wind-induced migration of Leddies in the South China Sea. J Phys Oceanogr. doi:10.1175/2011JPO4530.1 (in press)

Perry KL (2001) SeaWinds on QuikSCAT Level 3 Daily, Gridded Ocean Wind Vectors (JPL SeaWinds Project). Version 1.1, JPL Document D-20335. Jet Propulsion Laboratory, Pasadena

Qu T, Mitsudera H, Yamagata T (2000) Intrusion of the North Pacific waters into the South China Sea. J Geophys Res 105:6415–6424

Rio MH, Schaeffer P, Moreaux G, Lemoine JM, Bronner E (2009) A new mean dynamic topography computed over the global ocean from GRACE data, altimetry and in situ measurements. Poster communication at OceanObs09 symposium, 21–25 September 2009, Venice. Available on http://www.aviso.oceanobs.com/fileadmin/documents/data/products/ auxiliary/MDT_Cnes-CLS09_poster_Oceanobs09.pdf

Semtner J Jr, Chervin R (1992) Ocean circulation from a global eddy-resolving model. J Geophys Res 97:5493–5550

Shaw PT (1991) The seasonal variation of the intrusion of the Philippine Sea water into the South China Sea. J Geophys Res 96:821–827

Sheremet VA (2001) Hysteresis of a western boundary current leaping across a gap. J Phys Oceanogr 31:1247–1259

Sheu W, Wu C, Oey L (2010) Blocking and Westward Passage of Eddies in the Luzon Strait. Deep-Sea Res II 57:1783–1791. doi:10.1016/j.dsr2.2010.04.004

Wang D, Xu H, Lin J, Hu J (2008) Anticyclonic eddies in the northeastern South China Sea during winter 2003/2004. J Oceanogr 64:925–935. doi:10.1007/s10872-008-0076-3

Yuan D, Han W, Hu D (2006) Surface Kuroshio path in the Luzon Strait area derived from satellite remote sensing data. J Geophys Res 111:C11007. doi:10.1029/2005JC003412

Yuan D, Han W, Hu D (2007) Anti-cyclonic eddies northwest of Luzon in summer-fall observed by satellite altimeters. Geophys Res Lett 34:L13610. doi:10.1029/2007GL029401

Zhao W, Hou Y, Qi P, Ken-tang LE, Li MK (2009) The effects of monsoons and connectivity of South China Sea on the seasonal variations of water exchange in the Luzon Strait. J Hydrodyn 21:264–270